Real-time gas-correlation imaging employing thermal background radiation

Sandsten, J; Weibring, Petter; Edner, Hans; Svanberg, Sune

Published in:
Optics Express

DOI:
10.1364/OE.6.000092

2000

Real-time gas-correlation imaging employing thermal background radiation

Jonas Sandsten, Petter Weibring, Hans Edner and Sune Svanberg
Department of Physics, Lund Institute of Technology, P.O. Box 118, S-221 00 Lund, Sweden
Jonas.Sandsten@fysik.lth.se

http://www-atom.fysik.lth.se

Abstract: Real-time imaging of gas leaks was demonstrated using an IR camera employing outdoor thermal background radiation. Ammonia, ethylene and methane detection was demonstrated in the spectral region 7-13 µm. Imaging was accomplished using an optical filter and a gas-correlation cell matching the absorption band of the gas. When two gases, such as ammonia and ethylene, are absorbing in the same wavelength region it is possible to isolate one for display by using gas-correlation multispectral imaging. Results from a field test on a leaking gas tanker are presented as QuickTime movies. A detection limit of 200 ppm × meter for ammonia was accomplished in this setup when the temperature difference between the background and the gas was 18 K and the frame rate was 15 Hz.

OCIS codes: (040.3060) Detectors, infrared; (110.3080) Infrared imaging; (280.1120) Air pollution monitoring; (300.6340) Spectroscopy, infrared

References and links

1. T.J. Kulp, P.E. Powers and R. Kennedy, "Remote imaging of controlled gas releases using active and passive infrared imaging systems," in *Infrared Technology and Applications XXIII*, B.F. Andresen, M. Strojnik Scholl, eds., Proc. SPIE **3061**, 269-278 (1997).
2. S.-Å. Ljungberg, T.J. Kulp and T.G. McRae, "State-of the-art and future plans for IR imaging of gaseous fugitive emission," in *Thermosense XIX*, R.N. Wurzbach, D.D. Burleigh, eds., Proc. SPIE **3056**, 2-19 (1997).
3. C. Allander, P. Carlsson, B. Hallén, B. Ljungqvist and O. Norlander, "Thermocamera a macroscopic method for the study of pollution with nitrous oxide in operating theatres", Acta Anaesth. Scand. **25**, 21-24 (1981).
4. T.G. McRae and T.J. Kulp, "Backscatter absorption gas imaging: a new technique for gas visualization," Appl. Opt. **32**, 4037-4050 (1993).
5. J. Sandsten, H. Edner and S. Svanberg, "Gas imaging by infrared gas-correlation spectrometry," Opt. Lett. **21,** 1945-1947 (1996), http://www-atom.fysik.lth.se/JonasSandsten/GasCorrelationImaging.htm.
6. T.V. Ward and H.H. Zwick, "Gas cell correlation spectrometer: GASPEC," Appl. Opt. **14,** 2896-2904 (1975).
7. H.S. Lee and H.H. Zwick, "Gas filter correlation instrument for the remote sensing of gas leaks," Rev. Sci. Instr. **56**, 1812-1819 (1985).
8. H. Edner, S. Svanberg, L. Unéus and W. Wendt, "Gas-correlation lidar," Opt. Lett. **9,** 493-495 (1984).
9. P.S. Andersson, S. Montán and S. Svanberg, "Multi-spectral system for medical fluorescence imaging," IEEE J. Quant. Electr. **QE-23**, 1798-1805 (1987).
10. L.S. Rothman, C.P. Rinsland, A. Goldman, S.T. Massie, D.P. Edwards, J.-M. Flaud, A. Perrin, C. Camy-Peyret, V. Dana, J.-Y. Mandin, J. Schroeder, A. McCann, R.R. Gamache, R.B. Wattsin, K. Yoshino, K.V. Chance, K.W. Juck, L.R. Brown, V. Nemtchechin, P. Varanasi, The HITRAN molecular spectroscopic database: 1996 edition., J. Quant. Spectrosc. Radiat. Transfer **60,** 665-710 (1998).
11. M.L. Polak, J.L. Hall and K.C. Herr, "Passive Fourier-transform infrared spectroscopy of chemical plumes: an algoritm for quantitative interpretation and real-time background removal," Appl. Opt. **34**, 5406-5412 (1995).
12. P.L. Hanst, QASoft ´96, Database and quantitative analysis program for measurements of gases, Infrared Analysis Inc., Anaheim, Ca, 1996.
13. GRAMS/32, Array basic programming language, Galactic Industries Corp.

1. Introduction

Real-time gas imaging is of great interest in many contexts [1,2]. Inspection of leaks from chemical installations, petrochemical plants, tank farms or pipelines has economical,

#19020 - $15.00 US Received January 03, 2000; Revised February 08, 2000

environmental and security aspects. Easily deployable surveillance techniques for assessing sites of accidents involving gas tankers or trains are desirable for public safety considerations. In the indoor working environment, gas flow monitoring around air inlets and outlets, extraction hoods or local ventilation units is useful for optimizing the construction and adjustment of installations. Emissions of geophysical origin (volcanoes, geothermal installations or mines) as well as natural emanations of greenhouse gases from agriculture, swamps etc., are also interesting to assess. Useful spectroscopic absorption features of the molecules of interest occur in the visible or infrared spectral regions. The vibrational-rotational bands in the fundamental infrared region, 3700 cm^{-1} to 500 cm^{-1}, are particularly suitable for sensitive gas detection. While active monitoring of gases using lidar techniques is possible, range and imaging capabilities are limited. A passive system using ambient background radiation is more attractive for real-time imaging. In the present paper we demonstrate, as we believe for the first time, practical gas passive imaging with gas identification using a sensitive infrared camera combined with optical filter and gas cell correlation techniques. The method relies on simultaneous multi-spectral imaging and computer processing of the data. Results from a field test on a leaking gas tanker are presented.

Previous IR work has involved the use of heat blankets or IR illuminators to enhance the natural radiation level [3]. Scanning laser irradiation has been employed for close-range applications [4]. Recently, we demonstrated selective gas imaging using gas-correlation spectrometry for automatic gas identification, in a working environment scene employing added IR radiation [5]. The gas-correlation principle was originally introduced for line-of-sight monitoring and has later also been used in combination with lidar [6-8].

The virtue of the gas-correlation technique is the holistic discrimination between spectral frequencies with specific gas absorption and transparent areas, which is obtained by comparing a direct recording to a recording through an optically thick gas absorption cell. In our previous work we extended the principle to imaging by employing a technique for simultaneous multi-spectral recording using a specially designed split-mirror Cassegrainian telescope, allowing up to 4 geometrically similar but spectrally differently filtered images to be simultaneously recorded in the four quadrants of the 2D detector [9]. Two of the images were used, one direct image and one, which was filtered through a gas cell. Gas flows in an indoor working environment were visualized, but the IR camera employed, an Agema THV900 SW unit, had a sensitivity limit calling for the slight heating of the background scene using a 1000 W IR illuminator equipped with a reflector. Our present work has overcome some of the previous limitation by utilizing a more sensitive Agema THV900 LW system and more powerful image processing techniques to actually allow ambient thermal outdoor background radiation as the only illumination in real-time recordings at 15 frames/s. The special virtue of the gas-correlation technique is that it allows the separation of gases which have overlapping spectra (e.g. ammonia and ethylene). A proper IR wavelength window where the gases of interest absorb is chosen by a bandpass filter, but the high-resolution "holistic" filtering is performed by the optically thick correlation gas. The lay-out of the present paper is as follows. Detailed spectral considerations are presented in the next section, including a method to estimate gas concentration $\times$ length, followed by a description in Sect. 3 of the experimental arrangements used in the field measurements. Our data processing and dynamic gas flow presentation are discussed in Sect. 4, followed by a section presenting our results. Finally, we conclude with a discussion section with suggestions for technology improvements and future work.

2. Spectral consideration

By using remote infrared detection techniques most species, except homonuclear diatomic species, can be detected and quantified due to their unique infrared spectral properties in the wavelength region 3-13 μm [10]. In order to choose the optimal wavelength region for passive detection several factors have to be taken into account. The most important factors are atmospheric transmission (i.e. water and carbon dioxide absorption), background radiation

#19020 - $15.00 US Received January 03, 2000; Revised February 08, 2000

flux and the integrated oscillator strengths of the absorption lines of the species of interest. Fig. 1 shows a typical atmospheric transmission in the IR region, together with the spectral radiances of five blackbody radiators with normal background temperatures ranging from 273 K to 313 K. As can be seen, water and carbon dioxide absorption block part of the spectrum or limit the effective range of optical measurements. The region from 8-13 µm contains more water bands than the 3-4 µm region, but the background radiation is more than 30 times higher at normal terrestrial temperatures, i.e. 300 K. The strength of the absorption band of many species of interest is also considerable higher in the 8-13 µm region. Even though water interference in the 7-8.5 µm (1400-1200 cm^{-1}) wavelength region is severely affecting the signals, it is possible to utilize this region for measurements of methane, employing the gas-correlation technique.

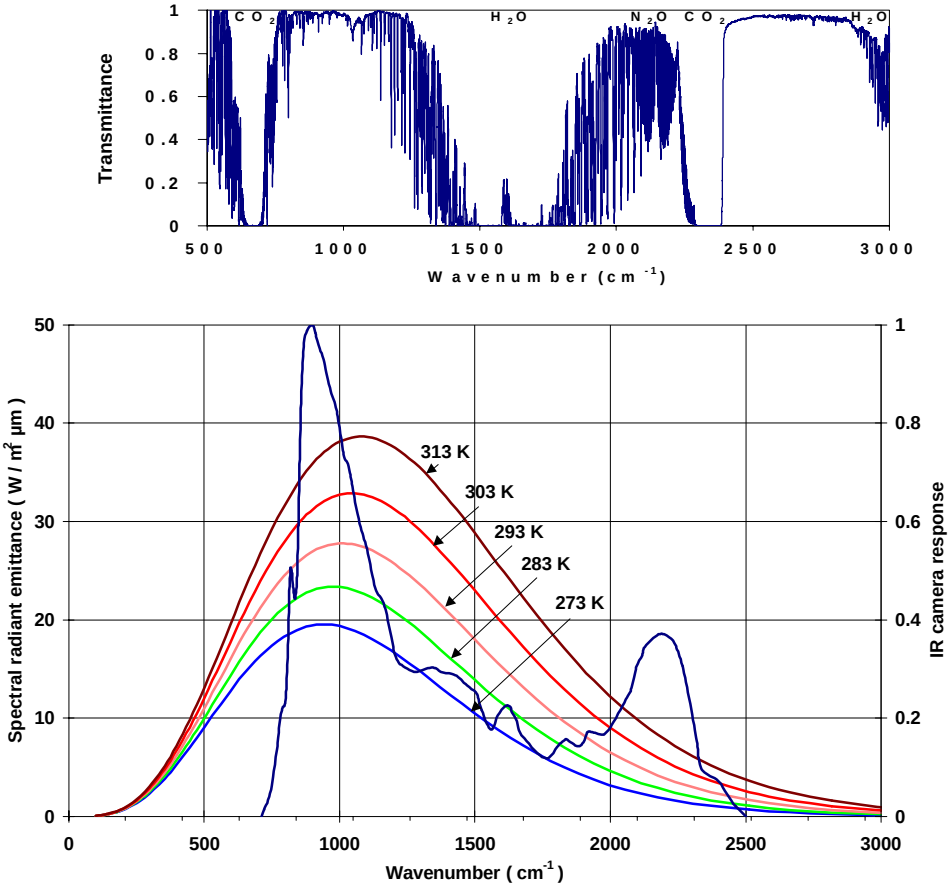

Fig. 1. Top: Atmosphere transmittance through 300 meters of urban air [12]. Bottom: Spectral radiance of five blackbody radiators (left axis) and the normalized spectral response curve of our IR camera (right axis).

Passive techniques using natural thermal background radiation for gas detection is very suitable around 1000 cm^{-1} due to maximum spectral radiance for such temperatures and a greatly transparent atmosphere. Gases that absorb infrared radiation in this atmospheric window are affecting the sun-earth radiative balance, which in turn is affecting the temperature on earth. IR cameras manufactured for use in the atmospheric window around 1000 cm^{-1}, are by definition also very suitable for visualization of greenhouse gas concentration gradients. Varying thermal background, reflectance or emittance over the image are compensated when using the imaging gas-correlation technique.

#19020 - $15.00 US
Received January 03, 2000; Revised February 08, 2000

Taken into account these spectral considerations we choose an Agema Thermovision 900 LW infrared camera, which has a low noise-equivalent temperature difference, NEΔT, of 80 mK. The relative spectral response, which is at its maximum at 900 cm^{-1} (11 µm), is also shown in Fig. 1. together with the spectral radiances of five blackbody radiators.

Computer based convolution simulations for the spectral response of the camera system, comprised of the detector, camera optics, filters and gas-correlation cells, were performed. The simulation enabled determination of the properties of the whole optical transmission system except the Cassegrainian telescope which was considered not to influence the spectral response notably. Also profiling and determination of different filter types were possible. To achieve an optimal sensitivity is a question of balancing the use of narrow bandpass filters, optimized on strong spectral features, to yield a high contrast response, against the overall photon transmission in the system. Static noise in the detector requires the photon flux to be over a certain level to achieve a good signal-to-noise ratio. Furthermore, a bandpass filter is in itself radiating more than a short- or long-wavelength-pass filter. Therefore, by varying the wavelength region and its width, maximizing the ratio between the integrated total absorption of the gas of interest and the integrated total optical transmission of the system, an optimal filter profile can be selected.

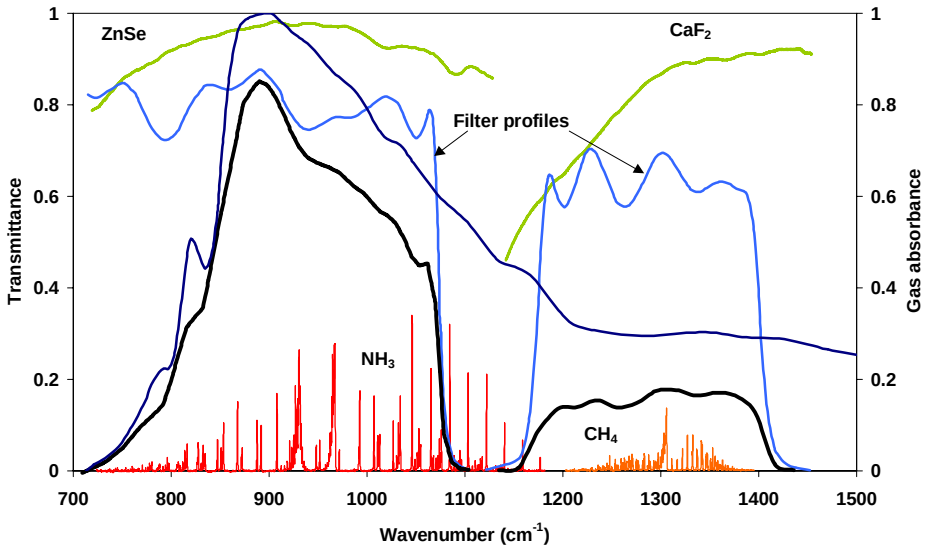

Fig. 2. The normalized spectral response of the IR camera (dark blue curve) is convoluted with the transmittance of two different gas cell window materials and optical filter profiles, yielding two regions of relative response (black curves). The gases are both shown in absorbance at concentrations of 200 ppm × m.

As a result of the simulations, a best effort filter for detection of ammonia and ethylene in the 8-13 µm wavelength region is a long-wavelength-pass filter (cut-on at 9.2 µm) with 80 % transmission and a best effort filter for detection of methane is a broad bandpass filter (half power points at 7 µm and 8.5 µm) with 60 % transmission.

For the gas-correlation cell windows, several materials with transmission in the 2-13 µm wavelength region were considered. We choose ZnSe for measurements of species with absorption around 10 µm, and CaF_2 for species around 8 µm; see Fig. 2. The ZnSe window surfaces were antireflection coated to reduce the reflection loss due to a high index of refraction, yielding more than 90 % transmission with a maximum of 99 % at 10.6 µm.

In Fig. 2 the transmittances of the discussed elements are shown together with the convoluted total response (black curves). FT-IR recorded spectra of 200 ppm × meters of ammonia and methane are shown in units of gas absorbance as red and orange lines, respectively [12].

#19020 - $15.00 US
Received January 03, 2000; Revised February 08, 2000

2.1 Gas concentration calibration

Gas concentration calibration for ammonia was performed by integrating the relative transmittance of the system over wavenumbers from 700 to 1100 cm^{-1}, with increasing gas concentrations, and then dividing the decreasing integrated relative transmittance with the integrated relative transmittance without gas. This procedure is primarily described for the case of direct absorption measurements. In the process the databases HITRAN 1996, QASoft '96 and the software GRAMS/32 were used [10,12,13]. Fig. 3 shows convoluted spectra at two different concentration levels. The absorption line wing contribution influence was taken into account by using HITRAN composite spectra.

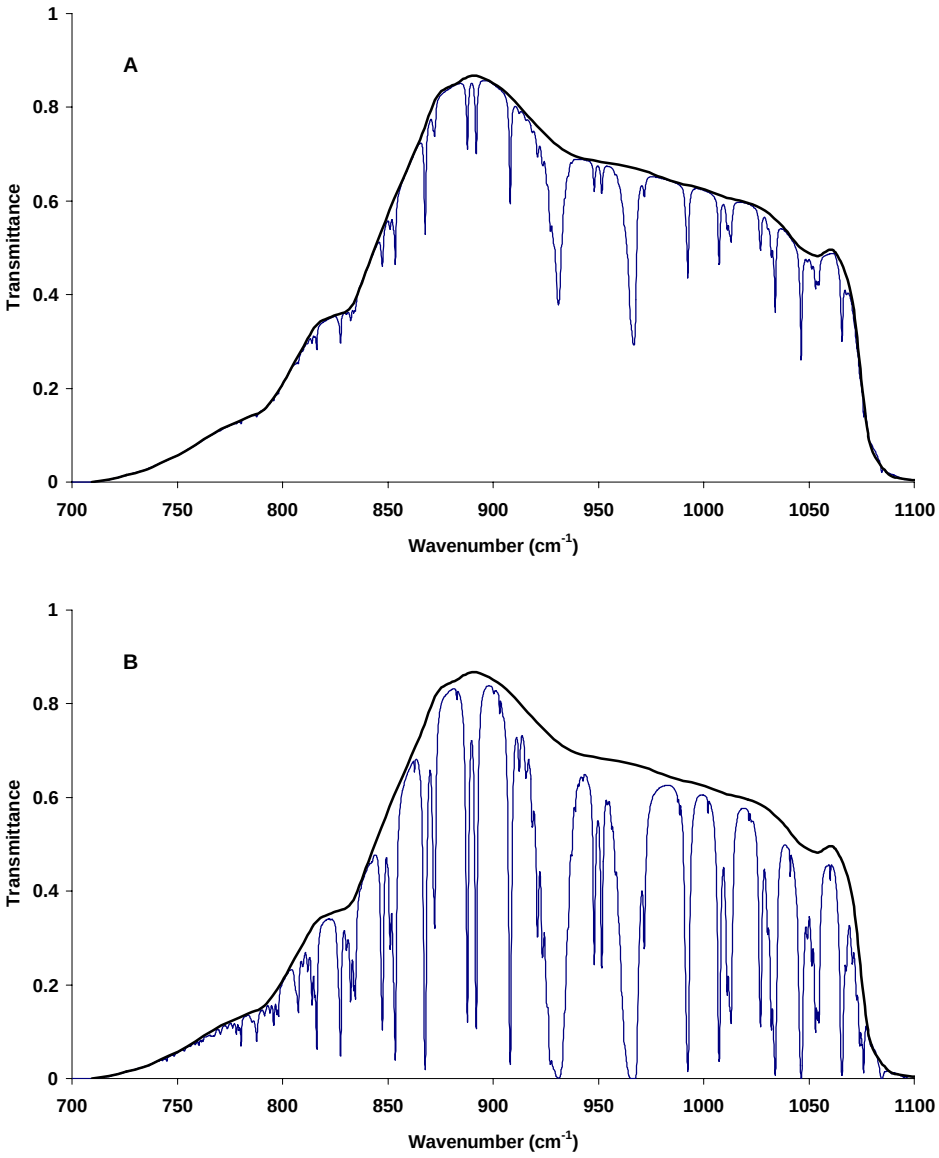

Fig. 3. A. Ammonia transmittance spectrum at a concentration of 400 ppm × m, convoluted with the system response. The black envelope integrated transmittance (no gas) divided by the integrated transmittance under the gas spectrum corresponds to the transmittance of the system. B. Ammonia transmittance spectrum at a concentration of 4000 ppm × m, convoluted with the system response.

#19020 - $15.00 US Received January 03, 2000; Revised February 08, 2000

Fig. 4 shows the integrated transmittance for different concentrations of ammonia, calculated from several convoluted spectra. This calculation was first performed for a very large temperature difference between the background and the gas. However, in a practical situation with a thermal background, the self-radiance from the gas has to be taken into account. The gas will selectively radiate at the absorption lines with an intensity of [(1-Transmittance) × B_G], where B_G is the intensity of a blackbody radiator at the gas temperature T_G. This will be seen as a higher effective transmittance of the gas, and this effect can be calculated by adding the emitted intensity of the gas at temperature T_G to the transmitted intensity of the background at temperature T_B. The resulting corrected transmittance as a function of the concentration at the prevailing experimental value of ΔT = 18 K ($\Delta T = T_B - T_G$) is shown in Fig. 4. We did not expect to find a Beer-Lambertian like relationship between gas transmittance and concentration since we have not monochromatic light, but a wavelength distribution requiring an extension of the law obtained by integration over wavenumbers. At small concentration levels we find a near linear relationship while going towards higher concentration levels the function becomes asymptotic. It should be noted that ΔT has to be known for a correct calibration and that for ΔT = 0 no absorption will be observed due to the fact that the absorption and emission cancel out.

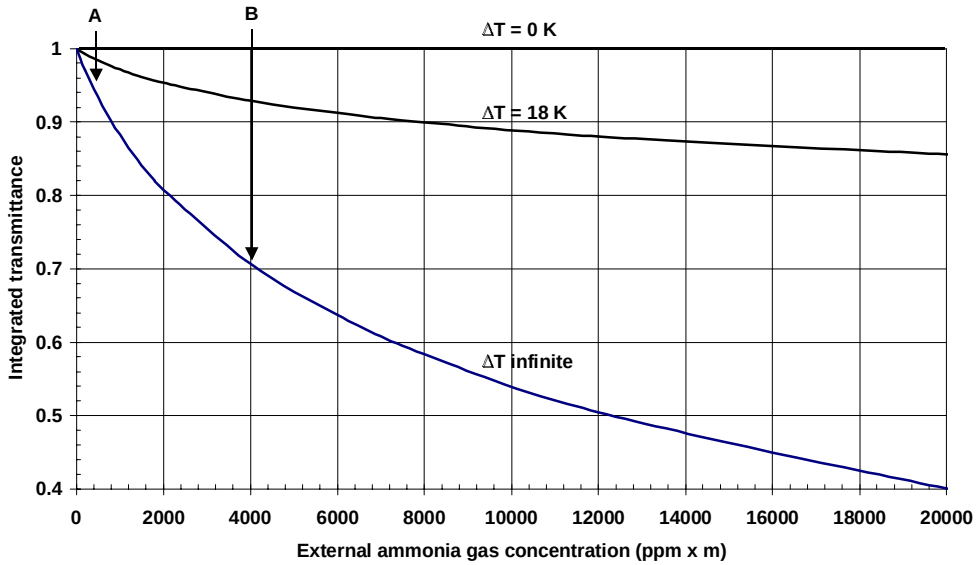

Fig. 4. Resulting calibrated ammonia gas concentration. Integrating the black envelopes in Fig. 3 corresponds to a transmittance value of one. Arrows A and B correspond to the integrated transmittance of the spectra in Fig. 3.

The theoretically calculated integrated transmittance values for different ΔT were validated in a laboratory set-up. A 8 × 8 cm^2 aluminum plate, coated with a high-emissivity black paint and coupled to a Peltier element, was used as the background target. In front of this a 20 mm thick cell filled with 20000 ppm × m ammonia gas was placed. The gas cell was held at a constant temperature of 294 K, while the temperature of the background target was varied. The results for 6 different values of ΔT are displayed in Fig. 5 together with the theoretical curve, showing good agreement. Please note, that for negative values of ΔT, a relative transmittance larger than 1 can be obtained. The temperature of the background surface was measured using a non-contact thermometer with laser aiming (Mikron® Instrument, model M101HT) with an accuracy of 1 K. The laboratory set-up was also used to determine the offset of the signal levels detected by the camera. This offset is mostly due to thermal emissions from the camera itself, the filter and the telescope. By plotting the detected

#19020 - $15.00 US Received January 03, 2000; Revised February 08, 2000

signal from the aluminum plate versus the band emittance from a blackbody at the measured temperature, the offset could be calculated.

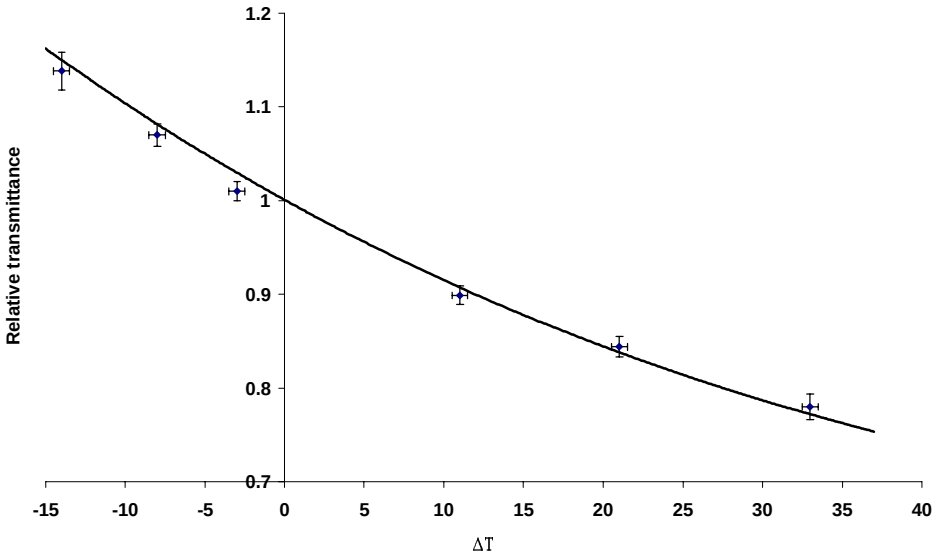

Fig. 5. Theoretically calculated relative transmittance through 20000 ppm × m ammonia gas as a function of $\Delta T = T_B - T_G$ with $T_G = 294$ K. The results of an experimental verification are inserted with error bars in the figure.

3. Field experiment arrangements

Field experiments with the techniques developed were performed at the training station of the Malmö Fire Brigade. This site is located in southern Sweden and the measurements were performed in the month of September during mostly sunny conditions with an ambient air temperature of 18-21 °C and a relative humidity of 50%. Rather windy conditions with gusts up to 12 m/s prevailed. The measurement scenario and optical arrangements are illustrated in Fig. 6. A burnt-out rusty gas tank trailer was used as the target, forming a background with a surface temperature of 30-40 °C and an emissivity of 0.9. Gas bottles with ammonia, ethylene and methane were connected through long tubes attached to the trailer, simulating leaks. This set-up enabled controlled releases of one or several gases with different flow rates at or near the ambient air temperature.

The optical equipment was placed at a distance of 20 m from the trailer. Two images of the object were formed at the same time on the IR-sensitive camera with the Cassegrainian split-mirror telescope, with a total receiving area of 2 × 10 cm^2. The all-reflective optics of the telescope are comprised of two primary spherical aluminum mirrors and a secondary spherical aluminum mirror. The aluminum with MgF_2 coating has 96% reflectance over the spectral region of the camera. The positions of the primary mirrors are adjustable by fine threaded screws and focusing is done by translating the secondary mirror along the common optical axis. The Agema Thermovision 900 LW camera is using a Stirling-cooled MCT signal-processing-in-the-element (SPRITE) detector and a scanner which, line by line, scans the object. Timing circuits create an image of the line scans resulting in a resolution of 272 × 136 pixels. The image is split by the Cassegrainian telescope into two regions of 136 × 136 pixels each.

#19020 - $15.00 US Received January 03, 2000; Revised February 08, 2000

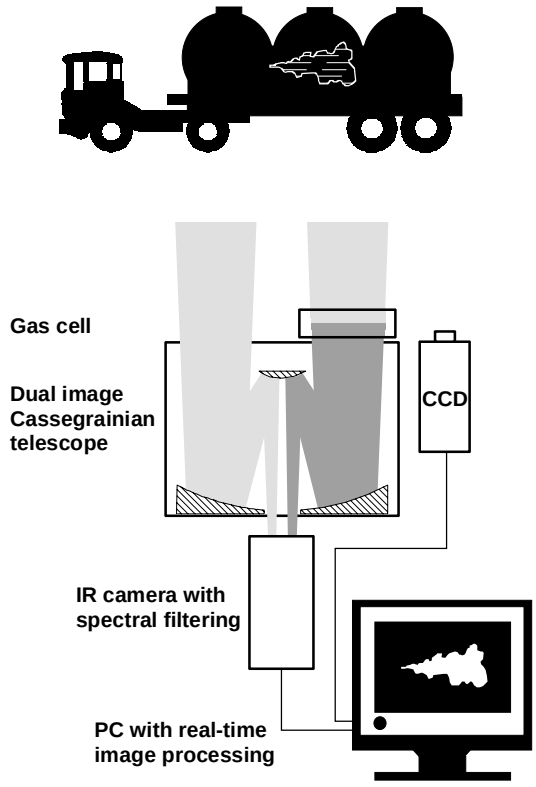

Fig. 6. Measurement scenario and optical arrangements.

The camera was equipped with suitable interference filters, used to isolate a small spectral region containing absorption features of the gas to be studied, as discussed earlier. The interference filters were mounted on a filter wheel in front of the detector inside the camera. In front of the telescope a 20 mm gas cell makes an additional filtering on one of the images. The gas cell was filled with an appropriate amount of a certain gas, making the cell essentially opaque at the stronger absorption lines. The two images thus produced can be used to extract a pure gas image and eliminate differences in the thermal background radiation as well as the interference by other gases or particles. A simultaneous recording of the scene in the visible spectral region was performed with a CCD camera mounted close to the telescope.

4. Data processing and dynamic presentation

The IR camera is connected to a PC with an Imaging Technology frame grabber and a fast SCSI hard disk, allowing real-time recordings of 12-bit, 272 × 136 pixels, at 15 frames/s. Image processing was performed on a PC with the Agema Irwin Research software and Matlab with the Image Processing Toolbox. After processing, the gas images could be overlaid on a normal image of the scene recorded with the CCD camera. The image processing was performed according to the following scheme:

- Two images A and B are captured at the same time using the Cassegrainian telescope, the IR camera and the frame grabber.
  A – image of the infrared scene from one of the telescope openings.
  B – image of the same scene with a gas cell in front of the other opening.
- The appropriate offset is subtracted from the images.
- An error (normalization) image, E, from the Cassegrainian telescope is created to handle imperfections such as asymmetrical vignetting, and stray-light from the two openings, $E = A_0 / B_0$. E is recorded with no gas present in the scene.

#19020 - $15.00 US Received January 03, 2000; Revised February 08, 2000

- The images are digitally overlapped by translation and optimization within a region of interest containing the gas, and subsequent image processing is restricted to this region.
- A gas-correlation image is calculated, G = A / B / E.
- On the result image, G a two-dimensional spatial median filter with a 3×3 neighborhood averaging is performed to reduce the strong spike-like noise components (salt-and-pepper noise).
- The concentration levels (of ammonia) are set by threshold values obtained from simulations in GRAMS/32 and calculations with Excel as described in Sect. 2.1.
- Finally, the gas-correlation image is overlaid onto a visible image of the background and the resulting 15 frames/s movie is presented in Matlab.

For presentation purposes QuickTime movies are created in which we electronically zoom into the gas leakage and compress the gas-correlation resulting movies for fast access on Internet. An additional advantage of the normalization procedure described above is that gas concentration evaluations for the case of gas-correlation imaging can be handled in a similar way as described for the direct absorption case in Fig. 4 and 5.

5. Measurements and results

Results from the measurements at the Malmö Fire Brigade gas training station are presented in three PC image processing modes; all of them based on the two-dimensional spectroscopic gas-correlation image processing. In Sect. 5.1 binary images of ammonia, ethylene and methane overlaid on a visible image of the gas tanker background are presented. In Sect. 5.2 the ammonia gas is presented together with a color-scale of the concentration overlaid onto the visible background image, and in Sect. 5.3 the ammonia gas is shown together with the spectrally interfering ethylene gas, but the ammonia gas is distinguished from the ethylene gas and colored red with the gas-correlation image processing mode.

5.1 Visualization of ammonia, ethylene and methane leaks

To the left in Fig. 7 we show one or more gases (green colored) which absorb infrared light from the background in the spectral region defined by the filter, cell window material and camera response. The right-hand image is the result of gas-correlation image processing and we are thus certain that the gas is ammonia (red colored) and not interfering gases or varying background reflectances, emissivities or temperatures. The gas correlation cell, with a length of 20 mm, was filled with ammonia at a pressure of 1 atm., resulting in 20000 ppm × meters with fully saturated spectral lines. It was not possible to detect external ammonia gas through the gas cell as expected.

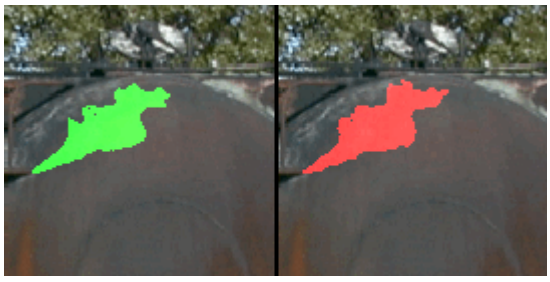

Fig. 7. (2 MB) Movie of an ammonia leak, left: by direct absorption and right: by gas-correlation. Binary gas images merged with visible images. Measurement conditions: Time 14:30, Air temperature 18 °C, Surface temperature 36 °C, Relative humidity 48 %, Gas flow 100 l/min, ZnSe gas cell with ammonia at 1 atm., Filter: Spectrogon LP9200.

In Fig. 8 we show leaking ethylene with the same method as for ammonia above. Again, we are certain that it is ethylene in the red-colored image due to gas correlation with an

#19020 - $15.00 US Received January 03, 2000; Revised February 08, 2000

ethylene gas cell. Notice that we have to somewhat sacrifice signal-to-noise ratio if we want to gain this information.

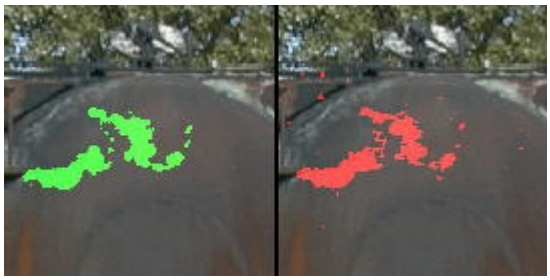

Fig. 8. (1.7 MB) Movie of an ethylene leak, left: by direct absorption and right: by gas correlation. Measurement conditions: Time 15:10, Air temperature 20 °C, Surface temperature 38 °C, Relative humidity 50 %, Gas flow 10 l/min, ZnSe gas cell with ethylene at 1 atm., Filter: Spectrogon LP9200

In Fig. 9 methane is visualized by direct absorption in the region from 7-8.5 µm which is very sensitive to water vapor, see Fig. 12. Water vapor interferes spectrally with methane gas but this problem is alleviated by gas correlation; the gas itself is the perfect spectral filter for discrimination against other gases. The lower sensitivity of the camera in this region gives a slightly lower signal-to-noise ratio.

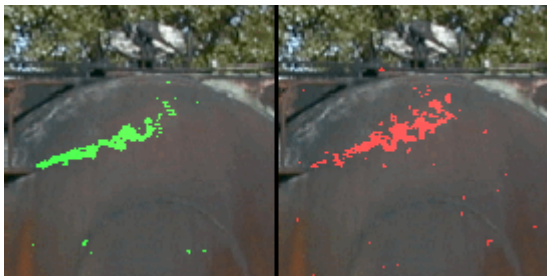

Fig. 9. (1.8 MB) Movie of a methane leak, left: by direct absorption and right: by gas correlation. Measurement conditions: Time 15:40, Air temperature 22 °C, Surface temperature 40 °C, Relative humidity 50 %, Gas flow 90 l/min, CaF_2 gas cell with methane 1 atm., Filter: Spectrogon BBP7040-8500

5.2 Ammonia gas concentration visualized with a concentration color-scale

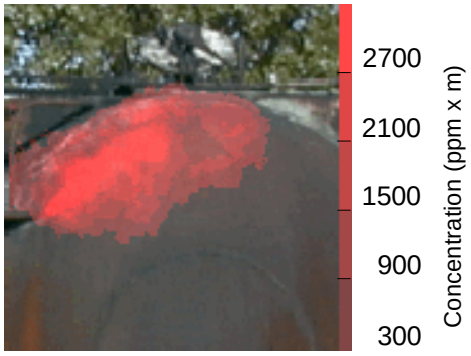

Fig. 10. (1.8 MB) Movie of an ammonia leak, color-scale concentration image. Measurement conditions: Time 14:30, Air temperature 18 °C, Surface temperature 36 °C, Relative humidity 48 %, Gas flow 10-100 l/min, ZnSe gas cell with ammonia at 1 atm., Filter: Spectrogon LP9200.

#19020 - $15.00 US
Received January 03, 2000; Revised February 08, 2000

The spatial two-dimensional concentration × length of ammonia, with an increasing flow from the first to the last image, is shown in Fig. 10. The concentration calculation was performed according to the method described in Sect. 2.1. This sequence of images was used to determine a detection limit of 200 ppm × m in the present set-up.

5.3 Spectrally interfering ammonia and ethylene separated by gas correlation

Fig. 11. (1.9 MB) Simultaneous imaging of ammonia and ethylene leaks showing the isolation of the ammonia flow using the gas-correlation technique. Measurement conditions: Time 17:25, Air temperature 19.2 °C, Surface temperature 31.5 °C, Relative humidity 50 %, Ammonia gas flow 15 l/min, Ethylene gas flow 10 l/min, ZnSe gas cell with ammonia 1 atm., Filter: Spectrogon LP9200.

In Fig. 11 the result of gas-correlation with ammonia and spectrally interfering ethylene is shown. The image on the left hand shows both ammonia (upper gas) and ethylene (lower gas) leaks in direct absorption and the image on the right hand is the result after gas correlation, showing ammonia only. We observe that a slight cross talk from ethylene is visible in some of the resulting ammonia frames; this is due to a few interfering spectral lines; see Fig. 12.

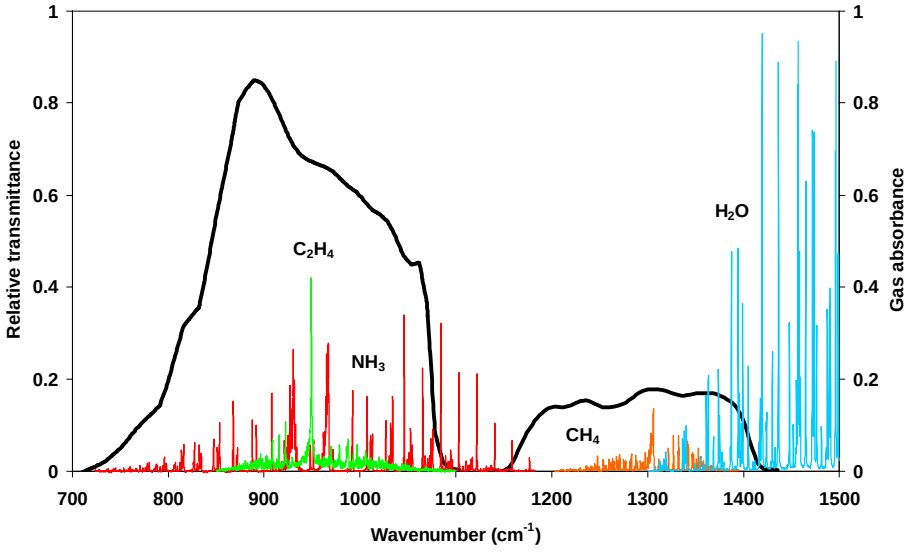

Fig. 12. Absorbance spectra of ammonia, ethylene and methane (200 ppm × m). Water vapor is interfering with methane. IR camera system relative response (black curves).

6. Discussion and conclusions

Real-time gas visualization using IR thermal background radiation and gas correlation is demonstrated, as we believe, for the first time. Live sequences of ammonia, ethylene and methane leaks are shown and gas separation for spectrally overlapping species is demonstrated. As shown in the paper there is a possibility to quantify the emissions. However,

#19020 - $15.00 US Received January 03, 2000; Revised February 08, 2000

an accurate knowledge of the temperature difference between the gas and the background is then necessary. Calibrated measurements also put a higher demand on control of the camera and telescope temperatures. Present sensitivities are in the range of 200 ppm × meters for ammonia (ΔT = 18 K) at a frame rate of 15 Hz, with an estimated sensitivity improvement of a factor 10 if moderate temporal and spatial averaging is performed. This detection limit is presently limited by imperfections in the telescope construction, resulting in image errors and varying offset problems. These effects could here be handled by recording an image without the gas present in the scene. With a better construction of the telescope, this procedure should not be necessary and the two sub-images, with and without the gas correlation cell, could be used to fully compensate for a varying background. Potentially, several gases could be monitored with a camera sensitive in the 8-14 µm region. The emerging QWIP (Quantum Well Infrared Photon) detector with tailored spectral sensitivities will clearly strongly improve future performance. The techniques presented have considerable potential for real-time monitoring of pipelines, even by helicopters, since the two images are captured exactly simultaneously, effectively eliminating spurious effects due to motion. Since the techniques rely on a temperature difference between the air and background temperature, it is important to select suitable time intervals for the monitoring [11].

Acknowledgements

The authors gratefully acknowledge interesting discussions with Sven-Åke Ljungberg, and the support of the Malmö Fire Brigade in performing the field experiments. Further, we are very grateful to Dr. Mats Kleverman of the Solid State Physics Division, LTH, for his kind help in performing the Fourier transform spectrometry recordings. This work was supported by the Swedish Space Board, the Swedish Engineering Sciences Research Council and the Knut and Alice Wallenberg Foundation.

#19020 - $15.00 US Received January 03, 2000; Revised February 08, 2000